Anal Bioanal Chem (2016) 408:3413–3423
DOI 10.1007/s00216-016-9415-1

RESEARCH PAPER

A miniaturized fiber-optic colorimetric sensor for nitrite determination by coupling with a microfluidic capillary waveguide

Yan Xiong[1,2] · Cheng-Jie Wang[1] · Tao Tao[1] · Ming Duan[1,2] · Shen-Wen Fang[1] · Min Zheng[1]

Received: 26 November 2015 / Revised: 26 January 2016 / Accepted: 10 February 2016 / Published online: 3 March 2016
© Springer-Verlag Berlin Heidelberg 2016

Abstract A microfluidic-capillary-waveguide-coupled fiber-optic sensor was developed for colorimetric determination of hazardous nitrite based on the Griess–Ilosvay reaction. The sensor was modularly designed by use of a light-emitting diode as the light source, silica fiber as the light transmission element, and a capillary waveguide tube as the light reaction flow cell. With the light interacting with the azo dye generated by the Griess–Ilosvay reaction between nitrite and Griess reagents, nitrite could be determined by a colorimetric method according to Beer's law. By use of the inexpensive and micro-sized elements mentioned above, the sensor provided a new low-cost and portable method for in situ and online measurement of nitrite. The sensor had a wide linear range for nitrite from 0.02 to 1.8 mg L^{-1} and a low detection limit of 7 μg L^{-1} (3σ), with a relative standard deviation of 0.37% (n = 10). With a low reagent demand of 200 μL, a short response time of 6.24 s, and excellent selectivity, the sensor is environmentally friendly and has been applied to nitrite determination in different water samples. The results were compared with those obtained by conventional spectrophotometry and ion chromatography, indicating the sensor's potential for practical applications.

✉ Ming Duan
swpua124@126.com

[1] State Key Laboratory of Oil and Gas Reservoir Geology and Exploitation, Southwest Petroleum University, Chengdu, Sichuan 610500, China

[2] Oil and Gas Field Applied Chemistry Key Laboratory of Sichuan Province, Southwest Petroleum University, Chengdu, Sichuan 610500, China

Keywords Fiber-optic colorimetric sensor · Nitrite determination · Microfluidic capillary waveguide · Griess–Ilosvay reaction

Introduction

With population increase and rapid economic growth, both severe water pollution and strict water safety requirements have become the focus of public attention. There is extensive concern worldwide about water pollution caused by nitrite (NO_2^-).

Nitrite is widely used in the production of food (as additives and preservatives), in industry (as dyes and bleaches), in agriculture (as fertilizers), and in physiological systems. However, it is a widespread inorganic pollutant and has been classified as a human health hazard. Many diseases are associated with high nitrite concentrations in drinking water. For example, methemoglobinemia (also called "blue baby syndrome" for infants) has been found to be caused by nitrite oxidizing hemoglobin to methemoglobin [1, 2]. Because of the nitrite oxidation effect, the oxygen-delivering capability of red blood cells is significantly reduced, and this may lead to death without proper treatment. A series of medical issues, including spontaneous abortions, intrauterine growth restriction, and birth defects of the central nervous system, have been ascribed to excess nitrite in drinking water by epidemiologic studies [3]. Furthermore, nitrogen fixation, denitrification, sedimentation, and many other anthropogenic processes which impact the quality of natural, surface, and underground waters are also closely associated with nitrite concentration [4, 5].

Because of the toxicity of nitrite, it has been recommended by the World Health Organization [6] and the US Environmental Protection Agency [7] that the maximum

contaminant levels of nitrite in drinking water should not exceed 3 mg L^{-1} and 1 mg L^{-1} respectively. Therefore, it is important to develop a highly efficient and reliable method for nitrite determination in water supplies to ensure a safe level.

A variety of different methods for nitrite determination have been developed, including spectrophotometry (e.g., absorption spectroscopy [8–11], fluorescence spectroscopy [12–14], and Raman spectroscopy [15]), electrochemistry (e.g., voltammetry [16, 17], potentiometry [18], impedimetry [19, 20], capillary electrophoresis [21], and electrode methods [22–24]), chromatography (e.g., ion chromatography [25], gas chromatography–mass spectrometry [26, 27], and high-performance liquid chromatography [28, 29]), and some other methods (e.g., kinetic methods and chemiluminescence [30–32]).

Among these techniques, use of an electrochemical system has become the most well-established method, but the electrochemical reaction is easily poisoned by sample constituents (e.g., H_2S, proteins, and certain anesthetics), and is not suitable for operation for prolonged periods in hostile and corrosive environments. Spectrophotometric absorption technology is commonly used as the standard nitrite determination method. The Griess–Ilosvay reaction [8–11, 33] has been the most popular color reaction used for nitrite absorption detection since 1879 [34]. It is generally based on nitrite reacting with a primary aromatic amine (e.g., sulfanilamide) under acidic conditions, leading to the formation of a diazonium salt, which further reacts with an aromatic compound containing an amino group (e.g., *N*-(1-naphthyl)ethylenediamine dihydrochloride) to form an intensely colored azo dye. However, the conventional colorimetric method commonly needs to use a spectrophotometer, which is not suitable for in situ and online measurements. As a result, the development of a portable, low-cost, and fast responding system is attractive for nitrite analysis.

During the past two decades, the development of a chemical sensor pushed the chemical analysis system to a new stage. It has been proven that a typical sensor can fulfill most steps in quantitative analysis [35–39] and provides an excellent strategy for species measurements with distinct advantages of fast analysis and easy portability [40–44].

A fiber-optic chemical sensor (FOCS) has been widely applied to species determination in the environmental, biological, and chemical fields [45–50]. It has distinguished advantages of simple manufacture, low cost, excellent electromagnetic interference resistance, and the possibility of remote analysis. Recently, to meet the demand of in situ and online measurements, much effort has been focused on the miniaturization of FOCS fabrication, leading to the development of microfluidic-capillary-waveguide-coupled micro FOCS methods.

The microfluidic capillary waveguide, which is a commonly used waveguide just like the planar waveguide, can be easily coupled with optical fibers and simultaneously act as a disposable sampling vessel, a reagent flow-through cell, and a light transmission element. As a result, the easily accessible microfluidic capillary waveguide is effectively available for FOCS miniaturization.

The present work aimed to design a novel miniaturized colorimetric FOCS system—that is, a capillary waveguide FOCS (CWFOCS)—for use in in situ and online measurement of hazardous nitrite based on the Griess–Ilosvay reaction. We designed the CWFOCS by coupling two ends of a microfluidic capillary waveguide with an excitation fiber and a emission fiber respectively. The excitation fiber was used to deliver the excitation light source into the capillary waveguide and the emission fiber was used to collect the light propagating from the capillary waveguide. When light propagated into the capillary waveguide through the excitation fiber, it could interact with the colored azo dye generated by the Griess–Ilosvay reaction in the microfluidic capillary waveguide. The intensity of the light would change with different nitrite concentrations and the light would propagate from the capillary waveguide through the emission fiber and into the detector. As a result, nitrite could be determined by a colorimetric method according to Beer's law. The sensor performances for nitrite detection have been evaluated in detail and the sensor was also applied to nitrite determination in real water samples. To validate the sensor's accuracy, sensitivity, and selectivity, the results obtained were compared with those obtained with the conventional methods of spectrophotometry and ion chromatography.

Experimental

Reagents and materials

We prepared the nitrite-sensitive Griess reagent by mixing the stock solution of 1 mg L^{-1} *N*-(1-naphthyl)ethylenediamine dihydrochloride (Sigma, USA), 50 mg L^{-1} sulfanilamide (Sigma, USA), and acetic acid (Kelong Chemical Reagent Company, China) according to a previously reported method [25]. The final solution was composed of 0.002% (w/v) *N*-(1-naphthyl)ethylenediamine dihydrochloride, 0.5% (w/v) sulfanilamide, and 14% (w/v) acetic acid.

Nitrite stock solution (100 mg L^{-1}) was prepared in water, and working solutions of nitrite were prepared freshly for daily use. All reagents were of analytical grade and were used as received. Wahaha® purified water (Wahaha, Hangzhou, China) was used for the preparation of the solutions and throughout the experiments.

Principle of the capillary-integrated fiber-optic sensor

In the simplest version, an optically transparent silica capillary could act as a waveguide. When the capillary's refractive index was higher than that of the sample medium (usually an aqueous solution) inside, the capillary could produce total internal reflection and then transport light from the light source (coupled with the exCitation fiber) to a detector (coupled with the detection fiber). In an ideal waveguide, light was conveyed in the medium of highest refractive index with virtually no loss.

When the sensing reagents flowed through the capillary flow cell, the colorimetric azo dye produced could function as an absorbing medium and interact with the light propagating into the capillary waveguide. As a result, the intensity of the propagating light would change with different nitrite concentrations and the nitrite could be determined by an absorption method according to Beer's law.

The power propagated by an optical capillary waveguide with its core locally replaced by an absorbing medium is given by [51]

$$P_L = P_0 \exp(-\gamma CL) \quad (1)$$

where P_L and P_0 are the power propagated through the capillary with and without an absorbing medium respectively. P_L and P_0 are proportional to I_L and I_0, which are the absorption intensity with and without an absorbing medium respectively. Therefore, with use of Beer's law, the "absorbance" defined in this work could be calculated as the relation between the intensity before and after the absorption process.

Design of the capillary-integrated fiber-optic sensor

One end of the excitation fiber (inner diameter 600 μm, Chunhui, Nanjing, China; *e*1′ in Fig. 1) was coupled with an LED light source (5 mm × 9 mm, Shifeng, China) by means of a homemade connector. One end of the emission fiber (inner diameter 600 μm, numerical aperture 0.37, Ocean Optics, USA; *e*2′ in Fig. 1) was coupled with a microspectrometer (QE65PRO, Ocean Optics, USA) by means of an SMA 905 connector (Ocean Optics, USA). The other ends of the excitation fiber (*e*1 in Fig. 1) and the emission fiber (*e*2 in Fig. 1) were coupled with the two ends of the capillary (inner diameter 1.6 mm).

The light could interact with the azo dye produced by the Griess–Ilosvay reaction between nitrite and Griess reagent in the capillary waveguide and propagated from the capillary waveguide to the detector. The light intensity changed with different nitrite concentrations, resulting in an absorbance change for colorimetric detection according to Beer's law. The distance from *e*1 to *e*2 was selected to be 10 cm to obtain the maximum absorbance detection efficiency; this distance was also considered to be equal to the length of the capillary flow cell.

Two peristaltic pumps were used to deliver samples and Griess reagent respectively. Water was used as a carrier and was delivered by a syringe pump. The solutions were injected by the sequential injection analysis system described in the next section. The whole design scheme is shown in Fig. 1.

Sequential injection analysis procedure

The flow-based method of sequential injection analysis is one of the universal solutions for the automation of analytical reactions. The equilibration in the reaction can be well achieved but dispersion of the reactants can be well prevented [52]. Generally speaking, sequential injection analysis is conceived to aspirate sample and reagent plugs sequentially through a selection valve toward a holding coil, and the plugs are directed to the detector by flow reversal.

In this work, the system was washed and filled with water carrier before the measurements were conducted. The analytical cycle began by aspiration of 60 μL of Griess reagent into the holding coil through port b of the multiselection valve (Fig. 1). Then 240 μL of sample solution was injected into the holding coil through port c. The entire volume was moved by a peristaltic pump in a counterclockwise direction at 100 μL s^{-1} through the reaction coil and then through the flow cell. At this stage, the response signal was measured at 540 nm by

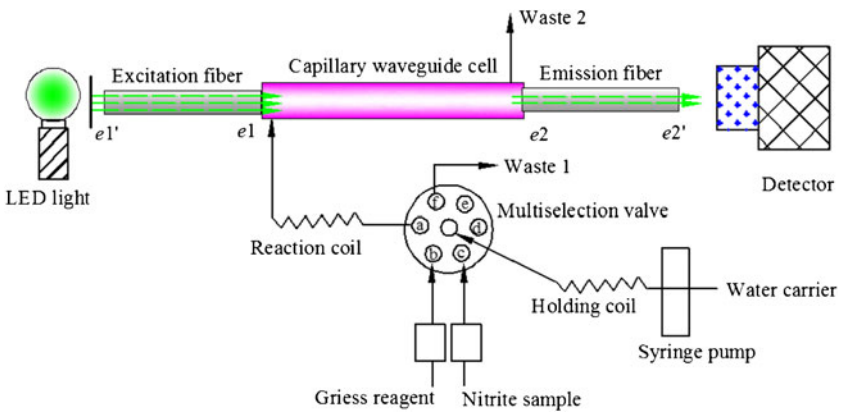

Fig. 1 The miniaturized fiber-optic colorimetric sensor for nitrite measurement

the detector, and system was washed with water. The detector signal corresponding to the baseline was measured with the same sequence of the operations. For this purpose, distilled water was used in place of the sample solution. The analytical signal was measured as a concentration peak.

Method comparison

UV–vis absorption

The UV–vis absorption determination of nitrite was performed with a UV-1800 spectrophotometer (Hitachi, Japan). We prepared a series of standards by mixing Griess reagent with different nitrite concentrations and they were used to prepare a calibration curve. Baseline zero was obtained with use of water, and samples were measured at 540 nm after zero absorbance had been set.

Ion chromatography

The ion chromatography determination of nitrite was performed with an 883 Basic IC plus ion chromatograph (Metrohm, Swiss) consisting of a high-pressure pump and a pulsed electrochemical detector, which was operated in the conductivity mode. Samples were separated on an IonPac anion-exchange column (250 mm × 4.0-mm inner diameter) coupled with a guard column (50 mm × 4.0-mm inner diameter). A Metrohm Anion micromembrane suppressor was installed between the conductivity detector and the separation column. The column was washed with eluent of 3.2 mmol L^{-1} Na_2CO_3 and 1.0 mmol L^{-1} $NaHCO_3$ solution with a flow rate of 0.7 mL min^{-1}. Ion suppression was accomplished with 5 mmol L^{-1} sulfuric acid with a flow of 0.7 mL min^{-1}.

Results and discussion

Spectral characteristics

To choose a low-cost commercial LED as an optimal light source for the sensor design, the absorption of Griess reagent and that of azo dye produced by the reaction between nitrite and Griess reagent were both measured. In Fig. 2a, spectrum 1 is the UV–vis absorption spectrum of Griess reagent and spectrum 2 is the UV–vis absorption spectrum of the azo dye used in the sensor. It can be seen that Griess reagent did not absorb in the UV–vis region. However, after it had reacted with nitrite, the azo dye produced had two obvious absorption peaks at λ_1 = 360 nm and λ_2 = 540 nm, which correspond to the violet color of R-band absorption and the green color of Q-band absorption respectively. Consequently, a green LED was chosen as the light source for the sensor design for two reasons. The first reason was that the absorption intensity at 540 nm was greater than that at 360 nm, which would lead to a more sensitive detection. The second reason was that the green LED with a visible spectrum was cheaper (only ¥0.5 per piece) than the violet LED with a UV spectrum, which could reduce the cost for sensor fabrication.

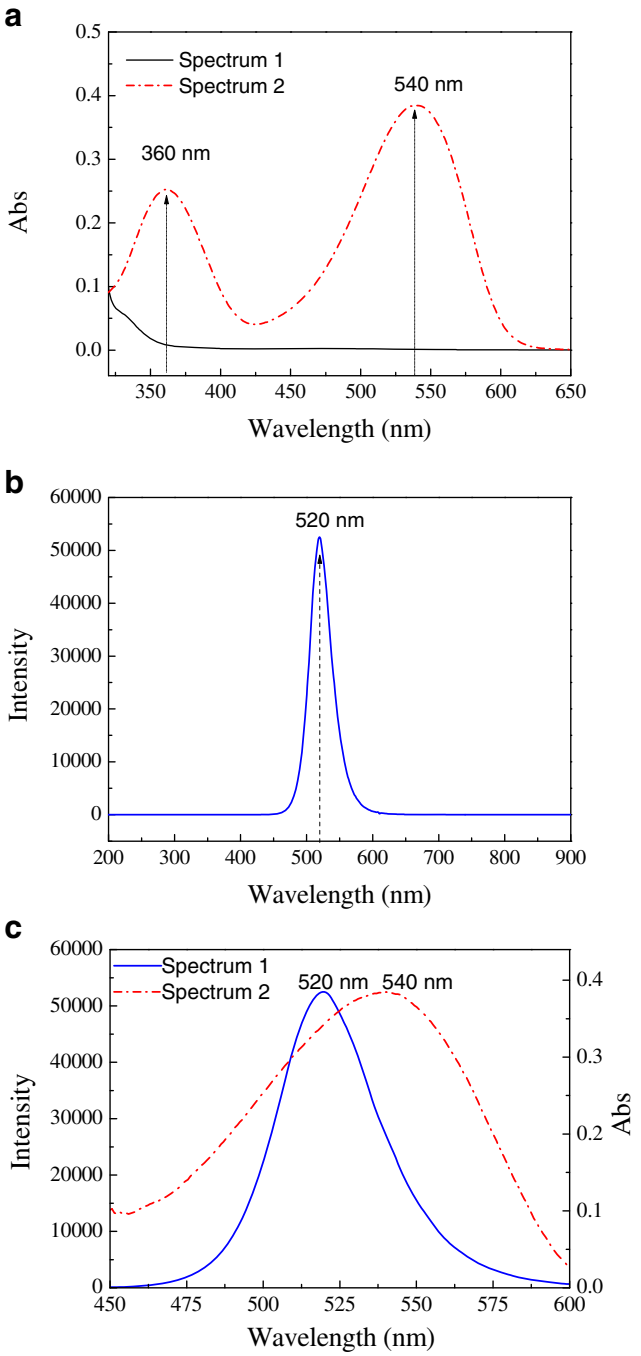

Fig. 2 Spectral characterization of the sensing system. **a** UV–vis absorption spectra of Griess reagent (spectrum 1) and the azo dye (spectrum 2). **b** Emission spectrum of the green LED light source chosen. **c** Overlapped spectra of the LED emission spectrum (spectrum 1) and the azo dye absorption spectrum (spectrum 2)

The green LED light source was then characterized. The emission spectrum of the LED was measured by the microspectrometer and is presented in Fig. 2b, which shows the emission wavelength centered at 520 nm. The LED emission spectrum (spectrum 1) overlapped and contrasted with the azo dye UV–vis absorption spectrum (spectrum 2) as shown in Fig. 2c. It can be seen that although there is a difference of 20 nm between the LED's emission peak and the azo dye's absorption peak, the emission spectrum of the LED still overlaps well with the absorption spectrum at 540 nm. This result confirmed our choice of the low-cost green LED as the excitation light source for the present colorimetric detection.

Optimization of sensor detection conditions

The prepared Griess reagent was used as a sensing reagent to react with nitrite samples. After a proper incubation time for the reaction between Griess reagent and the nitrite sample, the azo dye produced was carried through the microfluidic capillary cell and was detected for nitrite determination. To obtain the best analytical performance of the proposed sensor, three main operation conditions were studied in detail; they are described in the following sections.

Volume ratio

We studied different volume ratios of nitrite solution and Griess reagent from 6:1 to 1:5 by fixing the flow rate of the detection reagent at 50 μL s^{-1} and with an incubation time of 10 min. With a basic unit of 100 μL and a capillary flow cell volume of 200 μL (inner diameter 1.6 mm, length 10 cm), the volume of the azo dye produced (at least 200 μL) was enough to fill the capillary cell for absorption detection. As shown in Fig. 3a, although the volume ratio of 4:1 showed the largest absorption, the absorbance deviation was less that 2% between volume ratios of 4:1 and 3:1. To avoid reagent waste, a volume ratio of 3:1 was chosen as the optimum reaction ratio.

Incubation time

The incubation time for the reaction between Griess reagent and the nitrite sample had to be studied because too short a time was insufficient for sample reaction but too long a time would result in a waste of time. The effect of the incubation time on absorption determination was studied from 1.5 to 52 min. As shown in Fig. 3b, significant changes in the absorbance were not observed after 40 min. Therefore, 40 min was chosen as the optimal incubation time to obtain the best absorption.

Flow rate

By choosing 3:1 as the volume ratio and 40 min as the incubation time, we investigated the effect of the detection reagent flow rate from 20 to 80 μL s^{-1}. The results in Fig. 3c show that there was no obvious change in absorbance when the flow rate was increased from 20 to 80 μL s^{-1}. This indicates that the

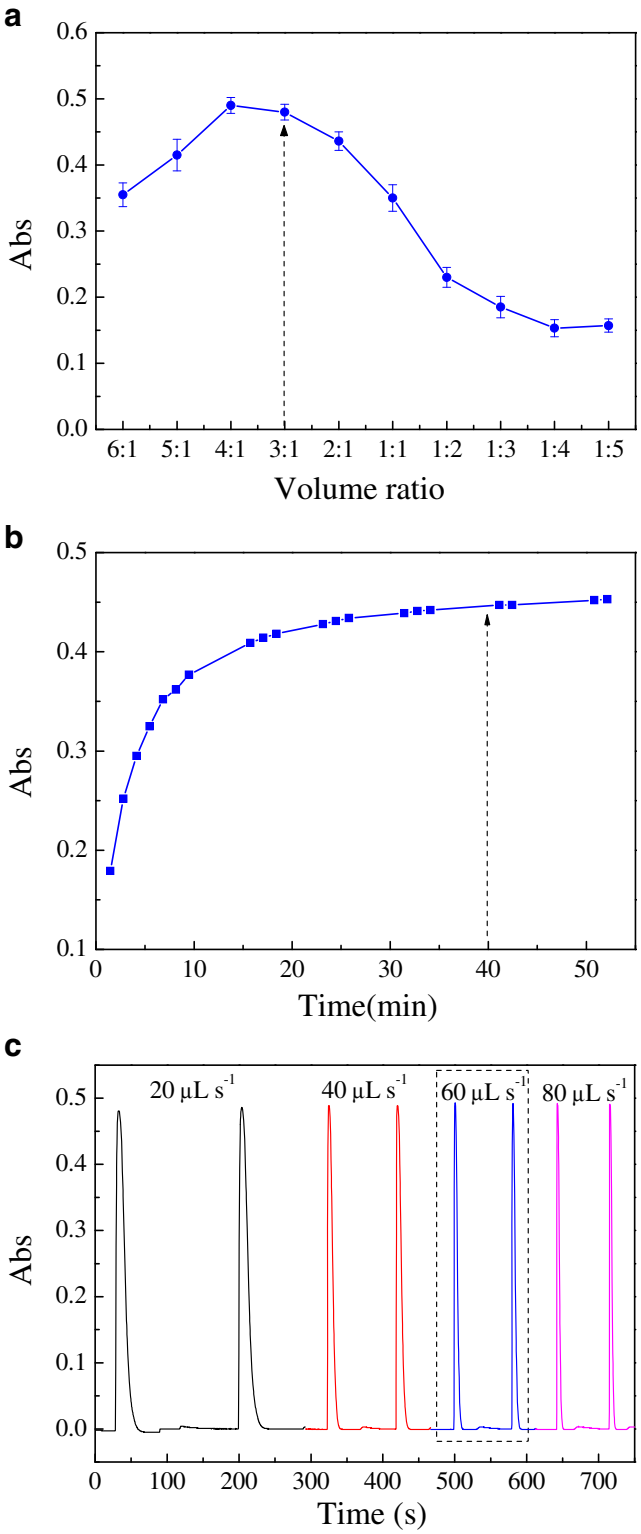

Fig. 3 Condition optimization of **a** volume ratio from 6:1 to 1:5 ($V_{nitrite}$/$V_{Griess\ reagent}$), **b** incubation time from 1.5 to 52 min, and **c** flow rate from 20 to 80 μL s^{-1}

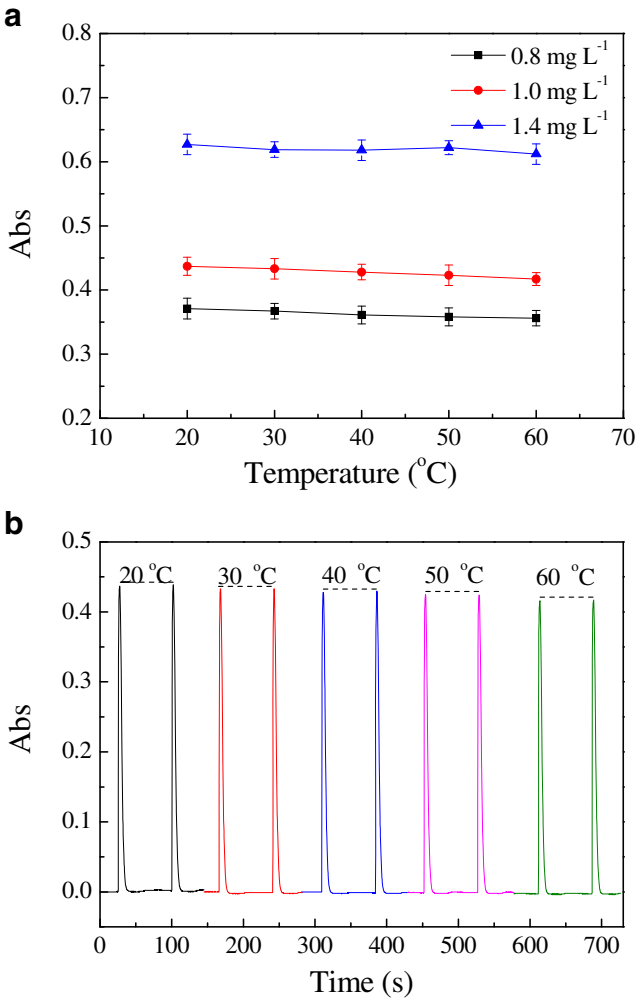

Fig. 4 Effect of temperature on sensor response: **a** different temperatures for different nitrite concentrations; **b** different temperatures for 1.0 mg L^{-1} nitrite concentration

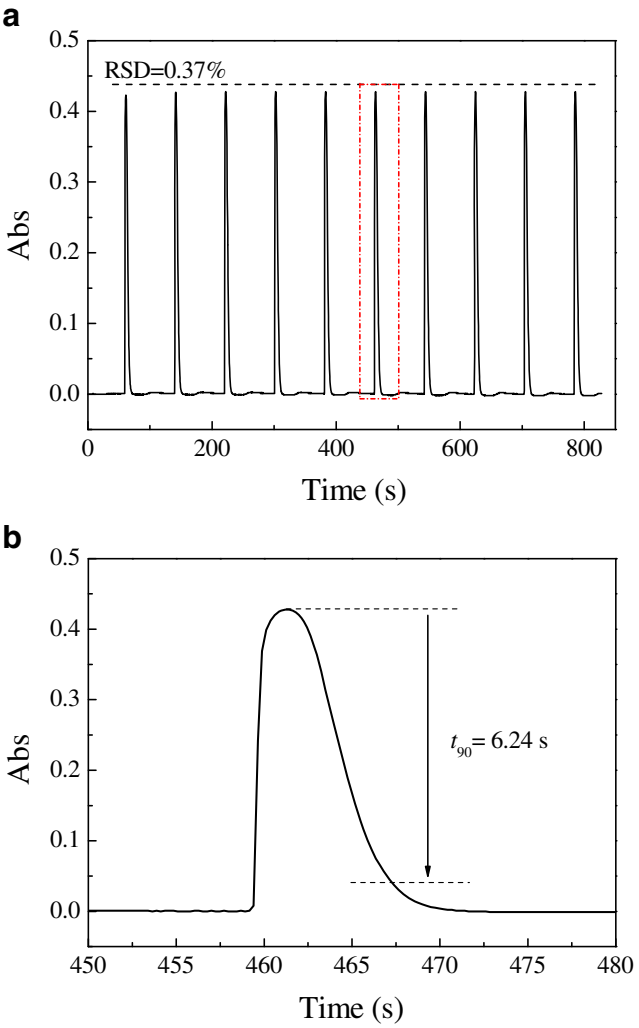

Fig. 6 **a** Typical repeatability measurement for nitrite at 1.0 mg L^{-1} with relative standard deviation (*RSD*) of 0.37%. **b** Typical dynamic measurement with response time of 6.24 s

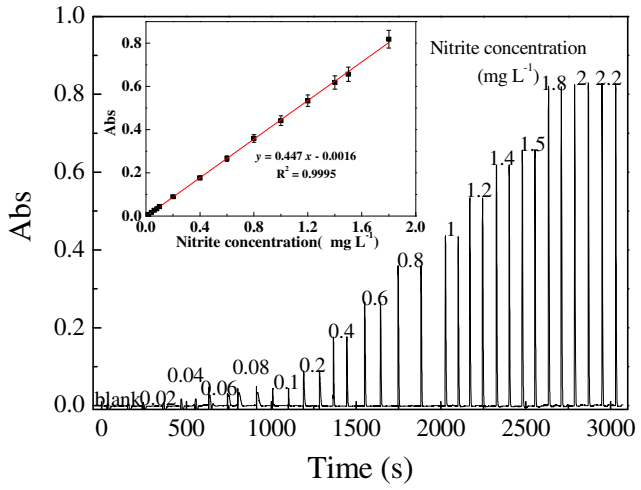

Fig. 5 Responses of the sensor to different nitrite concentrations. The *inset* shows the calibration curve

Table 1 Interference of foreign ions

Foreign ion	Tolerance limit (mg L^{-1})	RSD (%)
NO_3^-	730	0.37
Cl^-	1220	0.21
F^-	225	0.59
CO_3^{2-}	55	0.59
SO_4^{2-}	365	0.14
PO_4^{3-}	290	0.25
Fe^{3+}	35	0.22
Fe^{2+}	45	0.36
K^+	525	0.36
Cu^{2+}	50	0.47
Ca^{2+}	180	0.37
Mg^{2+}	125	0.20

RSD relative standard deviation

Table 2 Results of recovery tests on real samples

Sample[a]	Nitrite added (mg L^{-1})	Nitrite found[b] (mg L^{-1})	Recovery (%)	RSD (%)
1	0.00	0.015	-	0.0
	0.08	0.091	95	1.5
	0.20	0.212	98	0.6
2	0.00	0.00	-	0.0
	0.08	0.086	108	1.6
	0.20	0.218	109	1.0
3	0.00	0.042	-	3.3
	0.08	0.118	95	1.1
	0.20	0.247	103	1.1
4	0.00	0.00	-	0.0
	0.08	0.084	105	1.6
	0.20	0.205	102	0.6

[a] Sample 1 was lake water, sample 2 was tap water, sample 3 was repeated boiling water, and sample 4 was commercial drinking water.

[b] Results obtained with the proposed sensor, as the average of three determinations

flow rate had nearly no effect on absorption determination with enough azo reagent to fill the capillary detection cell. However, 60 μL s^{-1} was chosen as the optimum flow rate because it gave a shorter detection time but would not result in reagent waste.

Temperature influence

By choosing the optimal conditions as described above, we also investigated the influence of different temperatures on absorption determination for three different nitrite concentrations: 0.8, 1.0, and 1.4 mg L^{-1}. The temperature range was selected from 20 to 60 °C as it reflected the common working range required for nitrite determination in practical environments. The results in Fig. 4a indicate that the absorbance decreased slightly with increasing temperature, which showed that temperature calibration was needed for practical determination at different temperatures. However, for a nitrite concentration of 1.0 mg L^{-1} at different temperatures, the results in Fig. 4b show that a constant temperature throughout the incubation period leads to the same absorbance. As a result, standard solutions and nitrite samples should be at nearly identical temperature both in the reaction period and during detection.

Characterization of sensor performance

Calibration graph and detection limits

Under the selected conditions given in the previous sections, the results showed that the color of the azo dye produced by the reaction between nitrite and Griess reagent changed from pink to red with increasing nitrite concentration. Then it would become saturated for absorption determination after a nitrite concentration of 1.8 mg L^{-1}. As a result, the calibration curve

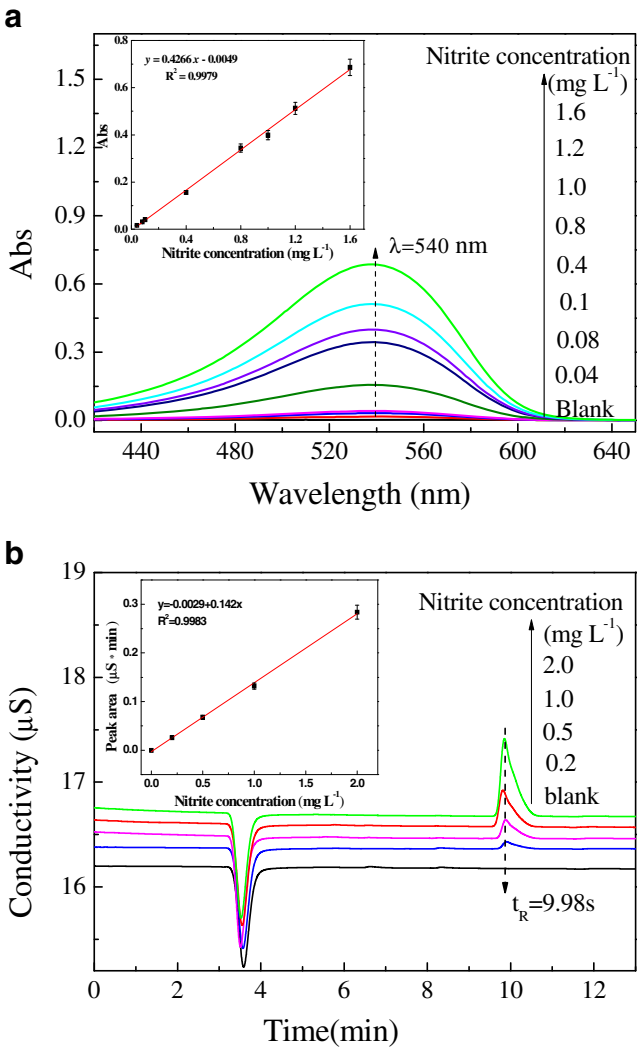

Fig. 7 Conventional methods for nitrite determination: **a** UV–vis absorption spectra; **b** ion chromatograms

Table 3 Performance comparison for three methods

Method	Linear range (mg L^{-1})	Correlation coefficient	LOD (mg L^{-1})	Reagent volume (mL)	Portability
Spectrophotometry	0.04-1.6	0.9979	0.02	4.0	No
Ion chromatography	0.2-2.0	0.9983	0.07	2.0	No
Presented sensor	0.02-1.8	0.9995	0.007	0.2	Yes

LOD limit of detection

was linear for nitrite concentrations in the range from 0.02 to 1.8 mg L^{-1} for the sensor. The typical absorption responses to different nitrite concentrations are shown in Fig. 5, and the linear calibration curve is shown in the inset. The calculated linear regression equation was y= 0.447x-0.0016, with a correlation coefficient of 0.9995, where y is the sensor response or absorbance and x is nitrite concentration.

The sensor's limit of detection was estimated to be 7 μg L^{-1} (3σ) for nitrite. This low detection limit was mainly contributed from two aspects. First, according to Beer's law, the absorbance was proportional to the capillary sensing length L as described in Eq. 1. So to obtain the maximum absorption detection efficiency, the sensing length of the optical fiber was selected to be 10 cm in this sensor design, which also matched the length of the capillary flow cell. Second, a microfluidic capillary waveguide with small inner diameter of 1.6 mm was used as the flow-through cell and sequential injection analysis was used as the chemical analysis technique. Both of these could effectively inhibit the sample dispersion caused by solution mixing and helped improve the sensor sensitivity. The detection limit obtained was enough for nitrite detection in a water sample, because the nitrite level recommended in drinking water is less than 1 mg L^{-1}.

Repeatability and response time

To validate the precision of the sensor, the repeatability of the sensor was tested by the analysis of a standard 1.0 mg L^{-1} nitrite solution ten times. The sensor's absorption response is shown in Fig. 6a, and the relative standard deviation was 0.37%.

The response time is an important parameter in sensor design and characterization. For many applications, a short response time is desirable. The response time in this study (t_{90}) was defined as the time required for a 90% change in the absorption reading from the equilibrium value. The experimental results are shown in Fig. 6b and indicate that t_{90} was 6.24 s under the selected conditions. Such a short response time was mainly a result of the small detection volume of the flow cell. For the fabricated sensor, the whole volume of the capillary flow cell was 200 μL, which could effectively speed up the solution displacement and was beneficial in shortening the response time.

Real sample analysis

To evaluate the overall selectivity of the proposed sensor, the influences of some ions that commonly exist in water were investigated for nitrite at 1 mg L^{-1} according to the recommended procedure. Interference was defined as a relative error of less than 5%. The results are shown in Table 1, where it can be seen that most of the ions tested did not interfere with determination.

Recovery was studied in four real water samples: lake water (sample 1), tap water (sample 2), repeated boiling water (sample 3), and commercial drinking water (sample 4). Samples 2 and 4 were directly tested without any pretreatment, but samples 1 and 3 were filtered through 0.45-μm Millipore filters before being tested. The recovery was determined by standard additions of a known amount of nitrite to water samples and was calculated from the typical standard calibration graph. The results in Table 2 show the recovery was in the range between 95 and 110%, indicating that the fabricated sensor had excellent accuracy.

Determination comparison

A comparison between the presented sensor and two conventional methods—UV–vis absorption spectroscopy and ion

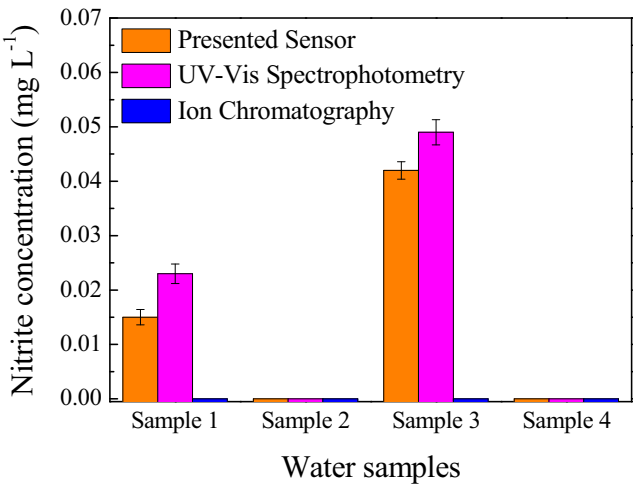

Fig. 8 Nitrite concentration in four water samples determined by three methods. (sample 1, lake water; sample 2, tap water; sample 3, repeated boiling water; sample 4, commercial drinking water)

chromatography—was conducted for nitrite determination from two aspects.

First, performance comparison for three methods was done. UV–vis absorption spectra and ion chromatograms for nitrite determination are illustrated Fig. 7. The results listed in Table 3 indicate that the sensor exhibited a wider linear range, a lower detection limit, and a smaller reagent volume. Furthermore, the sensor exhibited another advantage, portability, which is helpful for in situ and online nitrite measurements.

Second, nitrite determination in four real water samples—lake water (sample 1), tap water (sample 2), repeated boiling water (sample 3), and commercial drinking water (sample 4)—was tested by three methods. The results are shown in Fig. 8. It can be seen that the results obtained with the present sensor and UV–vis absorption spectroscopy were in agreement (relative error less than 10%), indicating that the proposed sensor is acceptable for practical use in most real water samples. However, the nitrite concentrations in these water samples were below the detection limit of the ion chromatography method, which indicated that the proposed sensor was more sensitive than ion chromatography.

Conclusions

In this work, a miniaturized fiber-optic colorimetric sensor was successfully developed for hazardous nitrite determination based on coupling with a microfluidic capillary waveguide. Compared with conventional methods for nitrite determination, this sensor shows several distinguished advantages.

First, small and inexpensive elements were used for sensor fabrication—for example, a capillary waveguide tube (inner diameter 1.6 mm) as the light reaction flow cell, silica fiber (inner diameter 0.6 mm) as the light transmission element, and an LED (5 mm × 9 mm) as the light source. As a result, this sensor is not only miniaturized to be portable for in situ and online measurement of nitrite, but also provides a new low-cost method for nitrite determination compared with the conventional high-cost spectrophotometry and ion chromatography.

Second, the microfluidic capillary waveguide simultaneously acts as a cell for the light reaction and sample detection, and as a disposable sampling vessel of defined volume in the present sensor fabrication. As a result, the sensor's sensitivity (limit of detection 7 μg L^{-1}) can be effectively enhanced and the response time (t_{90} = 6.24 s) can be greatly shortened because of the capillary's small inner diameter (1.6 mm) and microliter detection volume (200 μL). At the same time, reagent consumption can also be significantly reduced because of the microliter detection volume requirement (200 μL), which indicates the sensor is environmentally friendly and beneficial for practical application.

Furthermore, the sensor is modularly designed with three parts: a light source coupled with an excitation fiber, a capillary waveguide flow cell, and a detector coupled with a detection fiber. Because of the similarity and flexibility of the modular design, other hazardous species can be directly or indirectly measured if one simply changes the light source or sensing reagents. Consequently, this sensor is a helpful miniaturized colorimetric detection platform for the monitoring of other hazardous species.

Acknowledgments This work was supported by the Open Fund of State Key Laboratory of Oil and Gas Reservoir Geology and Exploitation (Southwest Petroleum University) (Grant No. PLN 1313), the National Natural Science Foundation of China (grant no. 51404203), the Foundation of Youth Science and Technology Innovation Team of Sichuan Province (grant no. 2015TD0007), and the Foundation of Science and Technology Department of Sichuan Province (grant no. 2014009).

Compliance with ethical standards

Conflict of interest The authors declare that they have no conflict of interest.

References

1. Greer FR, Shannon M. Infant methemoglobinemia: the role of dietary nitrate in food and water. Pediatrics. 2005;116:784–6. doi:10.1542/peds.2005-1497.
2. Jia L, Bonaventura C, Bonaventura J, Stamler JS. S-Nitrosohemoglobin: a dynamic activity of blood involved in vascular control. Nature. 1996;380:221–6. doi:10.1038/380221a0.
3. Brender JD, Olive JM, Felkner M, Suarez L, Marckwardt W, Hendricks KA. Dietary nitrites and nitrates, nitro stable drugs, and neural tube defects. Epidemiology. 2004;15(330):336. doi:10.1097/01.ede.0000121381.79831.7b.
4. Wolff IA, Wassennan AE. Nitrates, nitrites, and nitrosamines. Science. 1972;177:15–9. doi:10.1126/science.177.4043.15.
5. Nelieu S, Shankar MV, Kerhoas L. Phototransformation of monuron induced by nitrate and nitrite ions in water: contribution of photonitration. J Photochem Photobiol A. 2008;193:1–9. doi:10.1016/j.jphotochem.2007.05.027.
6. World Health Organization. Guidelines for drinking water quality, 3rd ed. Incorporating first and second addenda to third edition. Geneva: World Health Organization; 2008.
7. Environmental Protection Agency. National primary drinking water regulations: contaminant specific fact sheets, inorganic chemicals. Consumer version. Washington: Environmental Protection Agency; 2009.
8. Adarsh N, Shanmugasundaram M, Ramaiah D. Efficient reaction based colorimetric probe for sensitive detection, quantification, and on-site analysis of nitrite ions in natural water resources. Anal Chem. 2013;85:10008–12. doi:10.1021/ac4031303.
9. Lopez-Ruiz N, Curto VF, Erenas MM, Benito-Lopez F, Diamond D, Palma AJ, et al. Smart phone-based simultaneous pH and nitrite colorimetric determination for paper microfluidic devices. Anal Chem. 2015;86(19):9554–62. doi:10.1021/ac5019205.

10. Jayawardane BM, Wei S, McKelvie ID, Kolev SD. Microfluidic paper-based analytical device for the determination of nitrite and nitrate. Anal Chem. 2014;86(15):7274–479. doi:10.1021/ac5013249.
11. Daniel WL, Han MS, Lee J-S, Mirkin CA. Colorimetric nitrite and nitrate detection with gold nanoparticle probes and kinetic end points. J Am Chem Soc. 2009;131(18):6362–3. doi:10.1021/ja901609k.
12. Han J, Zhang C, Liu F, Liu B, Han M, Zou W, et al. Upconversion nanoparticles for ratiometric fluorescence detection of nitrite. Analyst. 2014;139(12):3032–8. doi:10.1039/c4an00402g.
13. Tabares LC, Kostrz D, Elmalk A, Andreoni A, Dennison C, Aartsma TJ, et al. Fluorescence lifetime analysis of nitrite reductase from Alcaligenes xylosoxidans at the single-molecule level reveals the enzyme mechanism. Chem Eur J. 2011;17(43):12015–9. doi:10.1002/chem.201102063.
14. Hong W-Y, Yang T-W, Wang C-M, Syu J-H, Lin Y-C, Meng H-F, et al. Conversion of absorption to fluorescence probe in solid-state sensor for nitric oxide and nitrite. Org Electron. 2013;14(4):1136–41. doi:10.1016/j.orgel.2012.12.011.
15. Zhang K, Hu Y, Li G. Diazotization-coupling reaction-based selective determination of nitrite in complex samples using shell-isolated nanoparticle-enhanced Raman spectroscopy. Talanta. 2013;2116:712–8. doi:10.1016/j.talanta.2013.07.019.
16. Turdean GL, Szabo G. Nitrite detection in meat products samples by square-wave voltammetry at a new single walled carbon naonotubes - myoglobin modified electrode. Food Chem. 2015;2179:325–30. doi:10.1016/j.foodchem.2015.01.106.
17. Wang Y, Laborda E, Compton RG. Electrochemical oxidation of nitrite: Kinetic, mechanistic and analytical study by square wave voltammetry. J Electroanal Chem. 2012;670:56–61. doi:10.1016/j.jelechem.2012.02.016.
18. Zarate N, Pilar Ruiz M, Perez-Olmos R, Araujo AN, Montenegro MCBSM. Development of a sequential injection analysis system for the potentiometric determination of nitrite in meat products by using a Gran's plot method. Microchim Acta. 2009;165(1–2):117–22. doi:10.1007/s00604-008-0107-1.
19. Labrador RH, Masot R, Alcaniz M, Baigts D, Soto J, Martinez-Manez R, et al. Prediction of NaCl, nitrate and nitrite contents in minced meat by using a voltammetric electronic tongue and an impedimetric sensor. Food Chem. 2010;122(3):864–70. doi:10.1016/j.foodchem.2010.02.049.
20. Zazoua A, Dernane C, Kazane I, Belghobsi M, Errachid A, Jaffrezic-Renault N. Gold electrode functionalized with catalase for impedimetric detection of nitrite. Sensor Lett. 2011;9(6):2283–6. doi:10.1166/sl.2011.1815.
21. Wang X, Adams E, Van Schepdael A. A fast and sensitive method for the determination of nitrite in human plasma by capillary electrophoresis with fluorescence detection. Talanta. 2012;97:142–4. doi:10.1016/j.talanta.2012.04.008.
22. Afkhami A, Soltani-Felehgari F, Madrakian T, Ghaedi H. Surface decoration of multi-walled carbon nanotubes modified carbon paste electrode with gold nanoparticles for electro-oxidation and sensitive determination of nitrite. Biosens Bioelectron. 2014;51:379–85. doi:10.1016/j.bios.2013.07.056.
23. Neel B, Asfhar MG, Crespo GA, Pawlak M, Dorokhin D, Bakker E. Nitrite-selective electrode based on cobalt(II) tert-butylsalophen ionophore. Electroanalysis. 2014;26(3):473–80. doi:10.1002/elan.201300607.
24. Wang L, Tricard S, Cao L, Liang Y, Zhao J, Fang J, et al. Prussian blue/1-butyl-3-methylimidazolium tetrafluoroborate Graphite felt electrodes for efficient electrocatalytic determination of nitrite. Sens Actuators B. 2015;214:70–5. doi:10.1016/j.snb.2015.03.009.
25. Wang N, Wang RQ, Zhu Y. A novel ion chromatography cycling-column-switching system for the determination of low-level chlorate and nitrite in high salt matrices. J Hazard Mater. 2012;2235:123–7. doi:10.1016/j.jhazmat.2012.07.029.
26. Tsikas D, Boehmer A, Mitschke A. Gas chromatography-mass spectrometry analysis of nitrite in biological fluids without derivatization. Anal Chem. 2010;82(12):5384–90. doi:10.1021/ac1008354.
27. Tsikas D, Schwarz A, Stichtenoth DO. Simultaneous measurement of [^{15}N]nitrate and [^{15}N]nitrite enrichment and concentration in urine by gas chromatography mass spectrometry as pentafluorobenzyl derivatives. Anal Chem. 2010;82(6):2585–7. doi:10.1021/ac902970m.
28. He L, Zhang K, Wang C, Luo X, Zhang S. Effective indirect enrichment and determination of nitrite ion in water and biological samples using ionic liquid-dispersive liquid-liquid microextraction combined with high-performance liquid chromatography. J Chromatogr A. 2011;1218(23):3595–600. doi:10.1016/j.chroma.2011.04.014.
29. Li Y, Whitaker JS, McCarty CL. Reversed-phase liquid chromatography/electrospray ionization/mass spectrometry with isotope dilution for the analysis of nitrate and nitrite in water. J Chromatogr A. 2011;1218(3):476–83. doi:10.1016/j.chroma.2010.11.073.
30. Lin Z, Xue W, Chen H, Lin J-M. Peroxynitrous-acid-induced chemiluminescence of fluorescent carbon dots for nitrite sensing. Anal Chem. 2011;83(21):8245–51. doi:10.1021/ac202039h.
31. Sui Y, Deng M, Xu S, Chen F. Gold nanocluster-enhanced peroxynitrous acid chemiluminescence for high selectivity sensing of nitrite. RSC Adv. 2015;5(18):13495–501. doi:10.1039/c4ra17164k.
32. Dong S, Guan W, Lu C. Quantum dots in organo-modified layered double hydroxide framework-improved peroxynitrous acid chemiluminescence for nitrite sensing. Sens Actuators B. 2013;188:597–602. doi:10.1016/j.snb.2013.07.060.
33. Czugala M, Fay C, O'Connor NE, Corcoran B, Benito-Lopez F, Diamond D. Portable integrated microfluidic analytical platform for the monitoring and detection of nitrite. Talanta. 2013;116:997–1004. doi:10.1016/j.talanta.2013.07.058.
34. Sun J, Zhang X, Broderick M, Fein H. Measurement of nitric oxide production in biological systems by using Griess reaction assay. Sensors. 2003;3:276–84. doi:10.3390/s30800276.
35. Chang I-H, Tulock JJ, Liu J, Kim W-S, Cannon Jr DM, Lu Y, et al. Miniaturized lead sensor based on lead-specific DNAzyme in a nanocapillary interconnected microfluidic device. Environ Sci Technol. 2005;39:3756–61. doi:10.1021/es040505f.
36. Austin DE. Miniaturization of analytical systems: principles, designs and applications. J Am Chem Soc. 2010;132:6864–5. doi:10.1021/ja102715s.
37. Zalesskiy SS, Danieli E, Blümich B, Ananikov VP. Miniaturization of NMR systems: desktop spectrometers, microcoil spectroscopy, and "NMR on a chip" for chemistry, biochemistry, and industry. Chem Rev. 2014;114:5641–94. doi:10.1021/cr400063g.
38. Merkoçi A, Kutter JP. Analytical miniaturization and nanotechnologies. Lab Chip. 2012;12:1915–6. doi:10.1039/C2LC90040H.
39. Lin S, Lee EK, Nguyen N, Khine M. Thermally-induced miniaturization for micro- and nanofabrication: progress and updates. Lab Chip. 2014;14:3475–88. doi:10.1039/C4LC00528G.
40. Chatterjee A, Khandare DG, Saini P, Chattopadhyay A, Majik MS, Banerjee M. Amine functionalized tetraphenylethylene: a novel aggregation-induced emission based fluorescent chemodosimeter for nitrite and nitrate ions. RSC Adv. 2015;5(40):31479–84. doi:10.1039/c4ra14765k.
41. Zhang R, Wang Y, Yu L-P. Specific and ultrasensitive ciprofloxacin detection by responsive photonic crystal sensor. J Hazard Mater. 2014;280:46–54. doi:10.1016/j.jhazmat.2014.07.032.
42. Wang S-Y, Ma J-Y, Li Z-J, Su HQ, Alkurd NR, Zhou W-L, et al. Surface acoustic wave ammonia sensor based on ZnO/SiO_2

composite film. J Hazard Mater. 2015;285:368–74. doi:10.1016/j.jhazmat.2014.12.014.
43. da Silva PS, Gasparini BC, Magosso HA, Spinelli A. Gold nanoparticles hosted in a water-soluble silsesquioxane polymer applied as a catalytic material onto an electrochemical sensor for detection of nitrophenol isomers. J Hazard Mater. 2014;273:70–7. doi:10.1016/j.jhazmat.2014.03.032.
44. Lee I, Oh W-K, Jang J. Screen-printed fluorescent sensors for rapid and sensitive anthrax biomarker detection. J Hazard Mater. 2013;252:186–91. doi:10.1016/j.jhazmat.2013.03.003.
45. Zhong N, Liao Q, Zhu X, Zhao M. Fiber Bragg grating with polyimide-silica hybrid membrane for accurately monitoring cell growth and temperature in a photobioreactor. Anal Chem. 2014;86:9278–85. doi:10.1021/ac502417a.
46. Zhong N, Liao Q, Zhu X, Chen R. A fiber-optic sensor for accurately monitoring biofilm growth in a hydrogen production photobioreactor. Anal Chem. 2014;86:3994–4001. doi:10.1021/ac500353y.
47. Ton X-A, Acha V, Bonomi P, Bui BTS, Haupt K. A disposable evanescent wave fiber optic sensor coated with a molecularly imprinted polymer as a selective fluorescence probe. Biosens Bioelectron. 2015;64:359–66. doi:10.1016/j.bios.2014.09.017.
48. Keller BK, DeGrandpre MD, Palmer CP. Waveguiding properties of fiber-optic capillaries for chemical sensing applications. Sens Actuators B. 2007;125:360–71. doi:10.1016/j.snb.2007.02.022.
49. Bao B, Melo L, Davies B, Fadaei H, Sinton D, Wild P. Detecting supercritical CO_2 in brine at sequestration pressure with an optical fiber sensor. Environ Sci Technol. 2013;47:306–13. doi:10.1021/es303596a.
50. Bagshaw EA, Wadham JL, Eveness J, Fountain AG, Telling J. Determination of dissolved oxygen in the cryosphere: a comprehensive laboratory and field evaluation of fiber optic sensors. Environ Sci Technol. 2011;45:700–5. doi:10.1021/es102571j.
51. Lee ST, George NA, Kumar PS, Radhakrishnan P, Nampoori VPN, Vallabhan CPG. Chemical sensing with microbent optical fiber. Opt Lett. 2001;26:1541–3. doi:10.1364/OL.26.001541.
52. Bulatov AV, Petrova AV, Vishnikin AB, Moskvin AL, Moskvin LN. Stepwise injection spectrophotometric determination of epinephrine. Talanta. 2012;96:62–7. doi:10.1016/j.talanta.2012.03.059.